FACULTY OF
MEDICINE,
DENTISTRY
& HEALTH
SCIENCES

FACULTY OF MEDICINE, DENTISTRY AND HEALTH SCIENCES

ST. VICENTS DEPARTMENT OF SURGERY

Articulated Kinematic Model of the Thoracic and Lumbar Spine

Model Building Methodology

Author:
Gino COATES

Supervisors:
A/Prof. P. PIVONKA,
A/Prof. A. BRYANT,
Dr. D. ACKLAND

30 Mar 2017

Contents

1 Introduction

This document details the development of an articulated lumbar and thoracic spine model suitable for kinematic analysis. The model uses the lumbar model by Christophy et al [2, 3] as a base, but has added custom joints to the thoracic spine segments. The lumbar vertebrae of the original model are already articulated, however the torso is a single fixed body connected to the L1 vertebra using a weld joint. Furthermore, the pelvis and sacrum are welded to the ground, preventing the models translation in 3D space. Finally, there is no limitation set on the range of motion of the inter-vertebral joints, meaning the range of movement cannot be clamped within the anatomical range for the joint. Using Christophy's model as a base, we performed the following modifications.

- Separated the thoracic vertebrae in the torso as separate bodies and added custom inter-vertebral joints.
- Applied ROM constraints for each inter-vertebral joint using a meta-analysis of data from the literature.
- Positioned the joints using the Instantaneous Axis of Rotation (IAR) from the study by Panjabi et al [8].
- Replaced the pelvis weld joint to the ground with a custom joint that allows translation in 3D space.
- Removed bodies that are not required for our study (e.g. Rib Cage).
- Added model markers on key bony landmarks such as the pelvis and spinous processes for scaling and IK purposes.

2 Methodology

The geometry of Christophy's lumbar spine model was digitized from a 25 year old male subject with a height of 170cm, and its posture was developed to be consistent with the average healthy human spine based on previous postural studies in the literature. We added a custom joint for each T segment with the following properties set;

- Location was set to (0 0 0)
- Location in parent was set to the origin of the Torso Joint in Christophy's model (0.0025 -0.089 0). This correctly positioned all of the bodies as per the original model
- The parent body was set to lumbar1.

- Range constraints were set for each joint as described later.

A C7 body and joint was added to the model that did not appear in Christophys lumbar model. However the C7 body was not correctly positioned with respect to the T vertebrae and need to be shifted accordingly to correct its position. Figure 1 illustrates the base model and the initial position of the C7 vertebra.

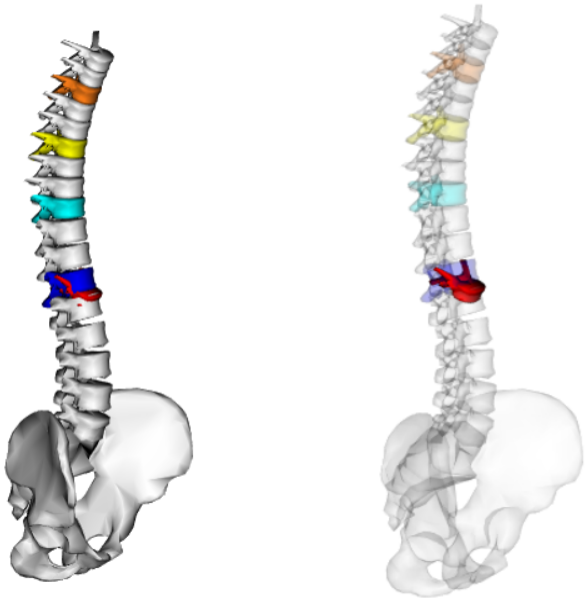

Figure 1: Base model (left). C7 vertebra added to the moddel (right)

Note that the same origin is shared by all T vertebrae in the base model. This was advantageous as it made it easy to calculate the IAR location with respect to both the child and parent geometry. On the other hand the C7 was not in the correct anatomical position and needed to be treated differently than the T segments. Figure 2 uses a marker positioned at 0,0,0 of the T11 and T12 and C7 bodies to indicate their difference in origin.

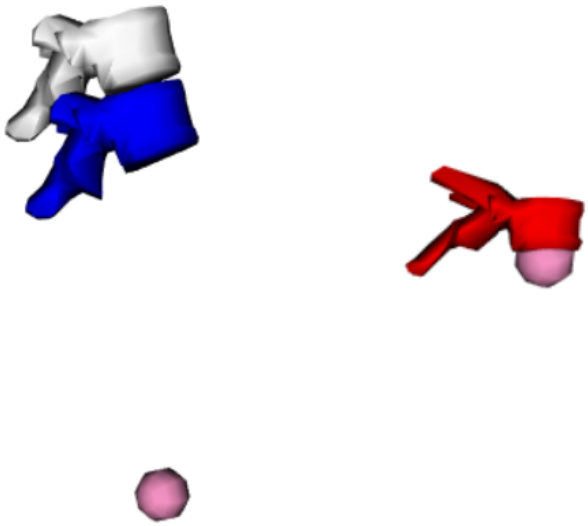

Figure 2: Origin of T12-L1 vertebra (left) and C7 vertebra (right)

3 Range of Motion Constraints

The range of motion of the thoracic segments has been set using a meta-analysis of the literature. We have applied maximum ROM for each motion segment based on various studies [4, 6, 7, 10, 11, 1, 9]. To apply a limit on the ROM of a joint, the range element has been set in radians on each joint coordinate as illustrated in Figure 3. The limit is applied by settings the ”clamp” element to true.

```
<Coordinate name="T9_T10_FE">
  <motion_type>rotational</motion_type>
  <default_value>8.67361737988404e-018</default_value>
  <default_speed_value>0</default_speed_value>
  <!--The minimum and maximum values that the
  coordinate can range between. Rotational coordinate range in radians
  and Translational in meters.-->
  <range>-0.062831853 0.041887902</range>
  <!--Flag indicating whether or not the values of the coordinates
  should be limited to the range, above.-->
  <clamped>true</clamped>
  <locked>false</locked>
  <prescribed_function />
  <prescribed>false</prescribed>
</Coordinate>
```

Figure 3: Joint range constraint applied to the the spine model T9 joint using the ”range” element.

Tables 1, 2, 3 list the applied range limits for lateral bending, flexion-extension and axial rotation respectively. For lateral bending and axial rotation the sum of the maximum ROM for each segment was taken and divided by 2 to give ROM in each direction. The calculated ROM for each section was then converted to radians.

Segment	Max	Left	Right	Radians (-ve)	Radians (+ve)
C7-T1	5	-2.5	2.5	-0.043633231	0.043633231
T1-T2	9	-4.5	4.5	-0.078539816	0.078539816
T2-T3	8.5	-4.25	4.25	-0.074176493	0.074176493
T3-T4	8.5	-4.25	4.25	-0.074176493	0.074176493
T4-T5	8.5	-4.25	4.25	-0.074176493	0.074176493
T5-T6	8	-4	4	-0.06981317	0.06981317
T6-T7	7	-3.5	3.5	-0.061086524	0.061086524
T7-T8	7	-3.5	3.5	-0.061086524	0.061086524
T8-T9	6.5	-3.25	3.25	-0.056723201	0.056723201
T9-T10	6	-3	3	-0.052359878	0.052359878
T10-T11	7	-3.5	3.5	-0.061086524	0.061086524
T11-T12	9	-4.5	4.5	-0.078539816	0.078539816
T12-L1	8	-4	4	-0.06981317	0.06981317

Table 1: Range of motion applied to the spine model for lateral bending

Segment	Max Flexion	Max Extension	Radians (-ve)	Radians (+ve)
C7-T1	9.4	-4.4	-0.076794487	0.16406095
T1-T2	3.6	-2.4	-0.041887902	0.062831853
T1-T2	3.6	-2.4	-0.041887902	0.062831853
T1-T2	3.6	-2.4	-0.041887902	0.062831853
T1-T2	3.6	-2.4	-0.041887902	0.062831853
T1-T2	3.6	-2.4	-0.041887902	0.062831853
T1-T2	3.6	-2.4	-0.041887902	0.062831853
T1-T2	3.6	-2.4	-0.041887902	0.062831853
T1-T2	3.6	-2.4	-0.041887902	0.062831853
T1-T2	3.6	-2.4	-0.041887902	0.062831853
T1-T2	3.6	-2.4	-0.041887902	0.062831853
T1-T2	3.4	-3.5	-0.061086524	0.059341195
T1-T2	5.5	-2.4	-0.041887902	0.095993109

Table 2: Range of motion applied to the spine model for flexion-extension

Segment	Max	Left	Right	Radians (-ve)	Radians(+ve)
C7-T1	8	-4	4	-0.06981317	0.06981317
T1-T2	9	-4.5	4.5	-0.078539816	0.078539816
T2-T3	8	-4	4	-0.06981317	0.06981317
T3-T4	8	-4	4	-0.06981317	0.06981317
T4-T5	8	-4	4	-0.06981317	0.06981317
T5-T6	8	-4	4	-0.06981317	0.06981317
T6-T7	8	-4	4	-0.06981317	0.06981317
T7-T8	8	-4	4	-0.06981317	0.06981317
T8-T9	7	-3.5	3.5	-0.061086524	0.061086524
T9-T10	6	-3	3	-0.052359878	0.052359878
T10-T11	7.5	-3.75	3.75	-0.065449847	0.065449847
T11-T12	9.5	-4.75	4.75	-0.082903139	0.082903139
T12-L1	10	-5	5	-0.087266463	0.087266463

Table 3: Range of motion applied to the spine model for axial rotation

4 Instantaneous Axis of Rotation

The IAR's for the lumbar region have already been set in Christophys base model based on previous studies in the literature (Figure 4).

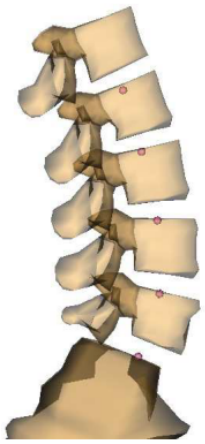

Figure 4: Locations of the axis of rotation in the thoracic vertebrae. a) IAR Location from Christophys Lumbar Model [2, 3]

We have selected the study by Panjabi et al to set the IAR of the thoracic region as it is the most systematic study found relating to the thoracic segments [8]. The authors determined the thoracic IAR from T1 to T12 in the saggital plane by applying six load types (Tension, Compression $\pm F_y$, Anterior/Posterior Shear $\pm F_x$, Flexion and Extension Moments $\pm M_x$) to the geometric center of the superior vertebral in each motion segment. Table 4 lists the IAR location results from Panjabi's study. In our model we have selected the location based on the $\pm M_x$ force type.

Load type	Observations	Cy	Cz	Dy	Dz
+Fy	48	-23.7	-2.8	116.6	221.9
-Fy	47	-29.2	-9.1	96.2	100.7
+Fz	51	-34.6	-0.6	36.0	17.7
-Fz	48	-46.6	-0.5	44.2	15.6
+Mx	54	-17.8	-0.0	48.9	18.6
-Mx	53	-17.8	-0.4	19.1	15.4

Table 4: IAR locations as per Panjabi et al[8]

Based on Panabi's results we selected an IAR for the T segments located at (0, -17.8, 0) with respect to the origin at the geometric center of the superior vertebra of a motion segment.

The C7 vertebra segment was not part of the original lumbar and needed to be correctly positioned before settings its IAR. We positioned the C7 body with respect to the T1 superior end-plate and the C7-T1 inter-vertebral disk height from the literature. Kunkel et al have measured the average centre disk height of the C7-T1 segment to be

3.6mm [5]. We assumed that the center of the inferior end-plate of C7 vertebral body should be aligned with the center of the superior end-plate of T1 vertebral body. We translated the C7 segment so that the distance between these points was 3.6mm, then calculated the location and location in parent points accordingly. Note that this gave us a C7 IAR close to the centre of the T1 body.

To find the geometric centre corresponding to the point of force application in Panjabi et al the center points of superior and inferior end-plates of each vertebral body were determined In Paraview 3D, a 3D visualization program that can read OpenSim vtp files. The vertices of interest were vertex 2 (inferior) and 110 (superior) respectively for each thoracic vertebral body. Figure 5 shows identification of the vertices of interest (pink dots). Note that in the base model provided by Christophy the thoracic segments are scaled to 0.87 their normal size, but in ParaView the body is unscaled. It's important to cater for this scaling difference when calculating the IAR positions.

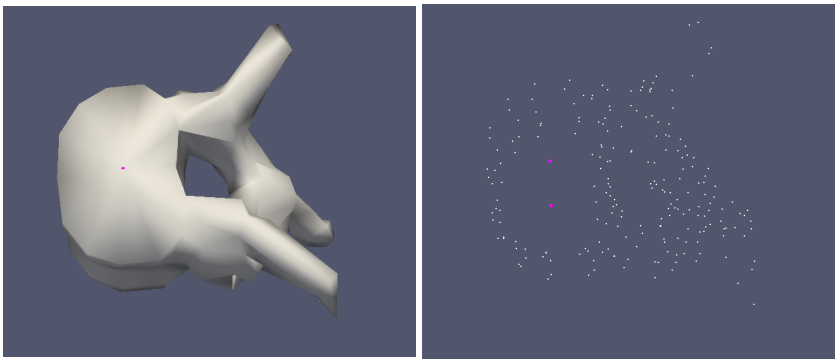

Figure 5: Identification of superir and inferior vertebral points (pink) in Paraview

Figure 6 illustrates the algorithm to calculate the IAR with respect to the superior and inferior points on the vertebral body. Given u is the superior end-plate center of the vertebral body and b is the calculated midpoint between the superior and inferior end-plate centers, and c is the IAR location that we want to find, then the IAR can be calculated as follows:

$$\bar{w} = \frac{(\bar{v} + \bar{u})}{2}$$
$$\bar{a} = \bar{w} - \bar{u}$$
$$|\bar{b}| = 1.78cm$$
$$\bar{c} = \bar{u} + \frac{\bar{a}}{|\bar{a}|} \cdot |\bar{a}| + |\bar{b}|$$

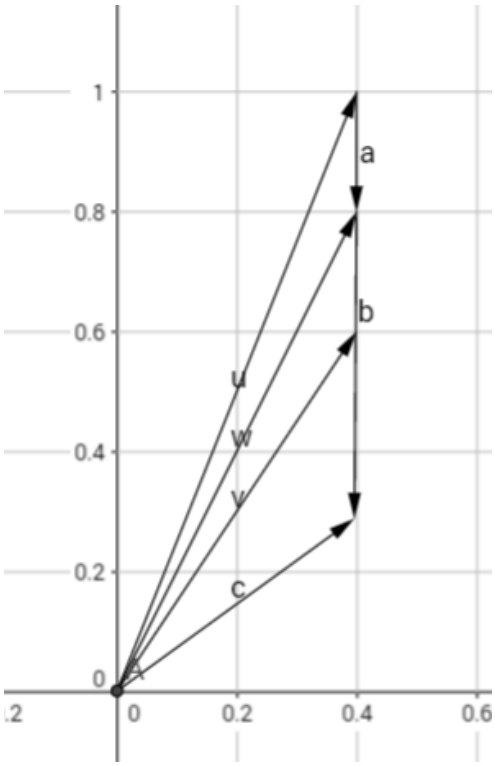

Figure 6: Graphical 2D representation of finding the IAR with respect to the center of the vertebral body

To maniplate the base model a custom Matlab script was developed. The steps to correct the T vertebrae were as follows. For each body:

- Translate the body using the offset of the original Torso joint in Christophys model [0.0025 -0.089 0]. This moves the origin of the T segment to correspond with the origin of the lumbar1 segment and maintains its correct anatomical position in the spine. The translation must be reverse scaled (i.e. by 2 - 0.87) as we are manipulating raw bodies in the matlab script and in the model the bodies are scaled to 0.87.
- Extract the superior and inferior end-plate center vertices of the vetebral body (vertices 110 and 2 respectively) from the vtp and scale them by 0.87.
- Calculate the IAR using the formula described above.
- Set the parent body appropriately (e.g. for T1 , T2 is the parent body).
- Set the location and location in parent of the joints to the calculated IAR. We set

both here as the parent and child bodies share the same origin and we want a ball joint located at the IAR position in the final model.

For the C7 segment we followed a similar approach to find the IAR, but first translated the body with respect the inter vertebral disk height, as described earlier.

5 Experimental Marker Placement

Model markers were attached to the spinous processes of the C7, T3, T6, T9,T12 and on the pelvis at the LPSI, RPSI and RIAC points. This was done programmatically in the model by positioning the markers adjacent to specific vertices that represent bony landmarks of interest for scaling and IK. The vertices were identified in Paraview as vertex 207 for the spinous processes, vertex 792 for the LPSI and RPSI landmarks and vertex 531 for the RIAC landmark. Figure 7 illustrates the position of these vertices in the bodies.

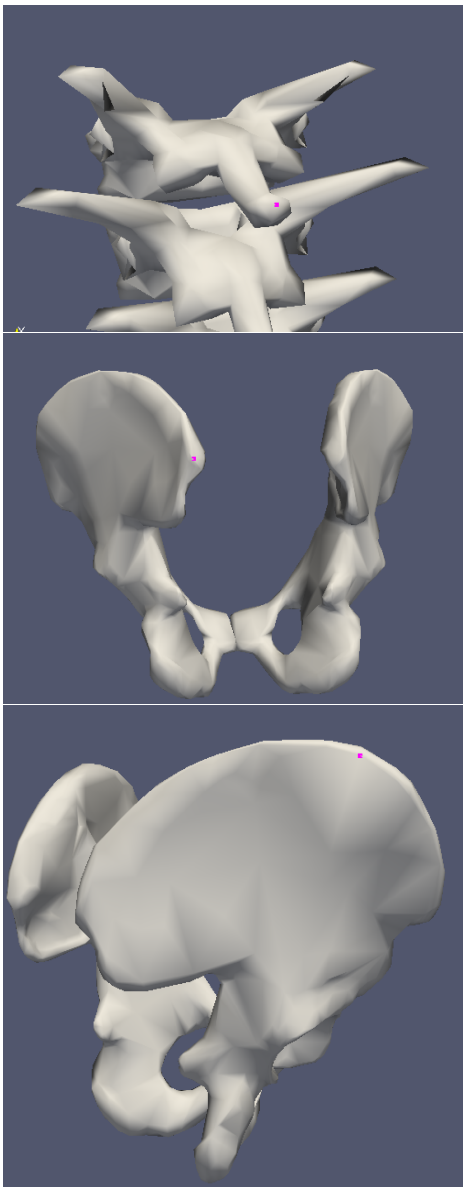

Figure 7: Selection of vertices (pink dot) for model marker placement. Spinous Processes (top), PSI (middle) and RIAC (bottom)

The experimental markers in use for our study are 38mm in size, so the Vertebral and PSI markers were be shifted by 1 radius (i.e 19mm) posterior to the bony landmark and the RIAC marker was shifted 1 radius to the right (+Z) of the iliac crest.

A custom matlab script was created to add markers to the model at the selected vertices. The process to add model markers was as follows:

- Extract the vertex of interest
- Scale the point to the scale size of the body in the model, for vertebral bodies this is 0.87, for Pelvis this is 1.0
- Offset the vertex in the appropriate direction. -X for the vertebral and PSI markers, +Z for the RIAC marker
- Add the model marker at the calculated point and label it accordingly

Note that in the base lumbar model by Christophy Lumbar the pelvis geometries are offset by [0.097 0.052 0], so this offset was also applied to position the model markers.

6 Results

Figure 8 shows the model in maximum flexion, extension and lateral bending. The poses were adopted by moving each of the thoracic vertetbrae to its maximum value for the plane of movement in the Open Sim coordinates window. Maximum ROM for the model in all planes of movement is presented in Table 5

Movement	Max ROM
Flexion	54.3°
Extension	-34.3°
Lateral Bending	±49°

Table 5: Model thoracic ROM in each direction

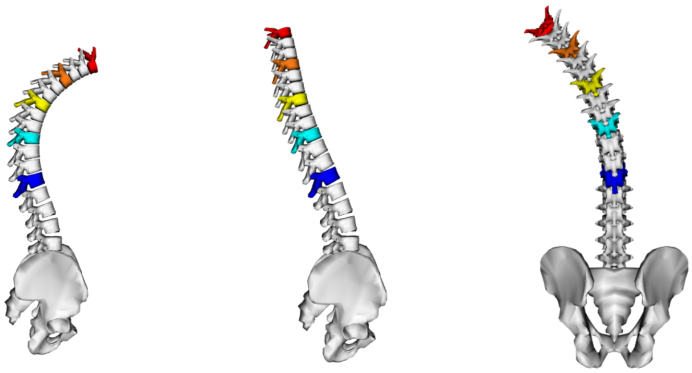

Figure 8: Range of motion of the model in maximum flexion (left), extension (middle) and lateral bending (right)

Figure 9 shows the final computed position of the IAR for the C7 to T12 vertebrae. To illustrate the computed position markers were added to each body at the IAR location.

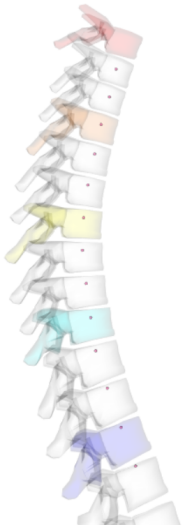

Figure 9: IAR position for the cervical and thoracic vertebrae

Figure 10 shows the final experimental markers added to the model at the selected bony landmarks. The markers are shown with sizes corresponding to the actual experimental marker sizes in use in our study.

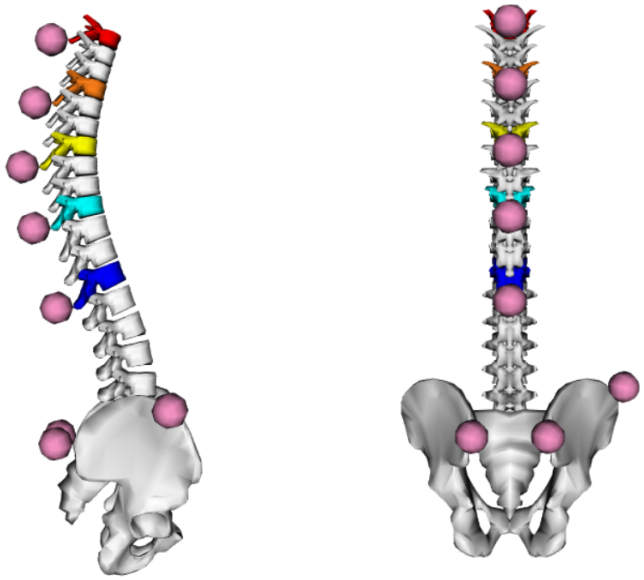

Figure 10: Final placement of the model markers

References

[1] W. J. Anderst, J. Y. Lee, W. F. Donaldson, and J. D. Kang. Three-dimensional intervertebral kinematics in the healthy young adult cervical spine during dynamic functional loading. *Journal of Biomechanics*, 48(7):1286–1293, 2015.

[2] M. Christophy. A Detailed Open-Source Musculoskeletal Model of the Human Lumbar Spine. 2010.

[3] M. Christophy, N. A. Faruk Senan, J. C. Lotz, and O. M. O'Reilly. A Musculoskeletal model for the lumbar spine. *Biomechanics and Modeling in Mechanobiology*, 11(1-2):19–34, 2012.

[4] E. Gercek, F. Hartmann, S. Kuhn, J. Degreif, P. M. Rommens, and L. Rudig. Dynamic angular three-dimensional measurement of multisegmental thoracolumbar motion in vivo. *Spine*, 33(21):2326–2333, 2008.

[5] M. E. Kunkel, A. Herkommer, M. Reinehr, T. M. Böckers, and H. J. Wilke. Morphometric analysis of the relationships between intervertebral disc and vertebral body heights: An anatomical and radiographic study of the human thoracic spine. *Journal of Anatomy*, 219(3):375–387, 2011.

[6] R. Louis. *Surgery of the spine : surgical anatomy and operative approaches*. Springer-Verlag, 1982.

[7] J. M. Morris. Biomechanics of the spine. *Archives of surgery*, 107(3):418–423, 1973.

[8] M. M. Panjabi, M. H. Krag, J. C. Dimnet, S. D. Walter, and R. a. Brand. Thoracic spine centers of rotation in the sagittal plane. *Journal of orthopaedic research : official publication of the Orthopaedic Research Society*, 1(4):387–394, 1984.

[9] a. a. White. Kinematics of the normal spine as related to scoliosis. *Journal of biomechanics*, 4(5):405–411, 1971.

[10] a. a. White 3rd and M. M. Panjabi. The basic kinematics of the human spine. A review of past and current knowledge, 1978.

[11] a. a. White 3rd, M. M. Panjabi, a. a. White 3rd, M. M. Panjabi, a. a. White 3rd, M. M. Panjabi, a. a. White 3rd, M. M. Panjabi, a. a. White 3rd, and M. M. Panjabi. The basic kinematics of the human spine. A review of past and current knowledge, 1978.